

¹⁴The names of the seventh and eighth quarks are from Greek seven (*hepta*) and eight (*oktō*). The fourth lepton f has been named to balance two Greek letters μ, τ with Roman e, f .

¹⁵To obtain the desired pattern of the symmetry breaking, one needs a cubic term in the potential. See Li, Ref. 8.

¹⁶M. S. Chanowitz, J. Ellis, and M. K. Gaillard, Nucl. Phys. **B128**, 506 (1977); H. Georgi and D. V. Nanopoulos, Nucl. Phys. **B155**, 52 (1979).

¹⁷Remember that the $\underline{1}$ of $[SU(2)]_H$ is the 2×2 antisymmetric matrix and the $\underline{3}$ is the symmetric matrix.

¹⁸M. Gell-Mann, P. Ramond, and R. Slansky, unpublished; E. Witten, Phys. Lett. **91B**, 81 (1980); R. N. Mohapatra and G. Senjanović, Phys. Rev. Lett. **44**, 912 (1980).

¹⁹M. Kobayashi and T. Maskawa, Prog. Theor. Phys. **49**, 652 (1973).

²⁰I. Bars and M. Günaydin, Phys. Rev. Lett. **45**, 859 (1980).

Measurement of Asymmetry in Spin-Dependent e - p Resonance-Region Scattering

G. Baum, M. R. Bergström, J. E. Clendenin, R. D. Ehrlich,^(a) V. W. Hughes, K. Kondo, M. S. Lubell, S. Miyashita, R. H. Miller, D. A. Palmer,^(b) W. Raith, N. Sasao,^(c) K. P. Schüler, and P. A. Souder
University of Bielefeld, D-4800 Bielefeld, West Germany, and Stanford Linear Accelerator Center, Stanford, California 94305, and University of Tsukuba, Ibaraki 300-31, Japan, and Yale University, New Haven, Connecticut 06520
 (Received 23 July 1980)

The first measurements are reported of the asymmetry in resonance-region scattering of longitudinally polarized electrons by longitudinally polarized protons. Data have been obtained at $Q^2 = 0.5$ and 1.5 (GeV/c)² in the missing-mass range $W = 1.1$ – 1.9 GeV. Results are compatible with a multipole analysis of single-pion electroproduction. The spin-dependent behavior is consistent with a duality mechanism as in the unpolarized case.

PACS numbers: 13.60.Hb

We have previously reported measurements of the asymmetry in spin-dependent elastic and deep-inelastic e - p scattering.¹⁻³ We report here the first resonance-region measurements⁴ of the asymmetry in the scattering of longitudinally polarized electrons from longitudinally polarized protons. Such data are of considerable interest to duality theory and to quark models of nucleon resonances, as well as to multipole analyses of electroproduction. Furthermore, we can learn how the scaling behavior of the spin-dependent structure function, which we have observed in the deep inelastic region,^{2,3,5} is approached at the rather small four-momentum transfers studied in this experiment.

The basic quantity determined is the asymmetry $A = [d\sigma(\uparrow\uparrow) - (d\sigma(\uparrow\downarrow))]/[d\sigma(\uparrow\uparrow) + d\sigma(\uparrow\downarrow)]$, in which $d\sigma$ denotes the inclusive differential cross section $d^2\sigma(E, E', \theta)/d\Omega dE'$ for electrons of incident (scattered) energy E (E') and laboratory scattering angle θ , and the arrows denote the antiparallel and parallel longitudinal spin configurations. The asymmetry A is obtained from the experimental asymmetry $\Delta = P_e P_p F A$, in which P_e is the electron-beam polarization, P_p is the proton-target polarization, and F is the fraction of detected

electrons scattered from the free (polarizable) protons in the complex target.

The experiment was performed at the Stanford Linear Accelerator Center with use of the 8-GeV/ c spectrometer and an experimental method reported previously.¹⁻³ The magnitudes of P_e and $\langle P_p \rangle$ were 0.85 ± 0.08 and 0.50 ± 0.04 , respectively, and F varied over the kinematic range from 0.08 to 0.21.

The kinematic points at which our measurements of Δ were made are listed in Table I. With $E = 6.47$ GeV and $\theta = 7.0^\circ$, five different momentum settings of the spectrometer from $E' = 4.92$ to 5.83 GeV covered continuously the missing-mass region W from 1.090 to 1.872 GeV for $Q^2 \approx 0.5$ (GeV/c)². With $E = 9.71$ GeV and $\theta = 8.0^\circ$, two E' settings of 7.87 and 8.13 GeV continuously covered the region $W = 1.360$ to 1.840 GeV for $Q^2 \approx 1.5$ (GeV/c)².

Radiative corrections associated with elastic and inelastic scattering are calculated by the same methods as those employed for deep-inelastic asymmetry data.^{3,6} The effect of the elastic tail is removed by expressing the inelastic asymmetry, A^{ine} , in the form $A = f^{\text{ine}} A^{\text{ine}} + f^e A^e$, where A^e is the calculated elastic asymmetry¹ and f^{ine}

TABLE I. Electron asymmetry data and elastic tail subtraction.

W (GeV)	Q ² (GeV/c) ²	E (GeV)	θ (deg)	Δ (%)	A (Measured electron asymmetry)	A _{efe}	f ^{ie} (Inelastic fraction)	A ^{ie} (Electron asymmetry after elastic tail subtraction)
1.168	0.57	6.47	7.0	0.127 ± 0.148	0.031 ± 0.035	0.049 ± 0.001	0.46	-0.030 ± 0.073
1.247	0.56	6.47	7.0	-0.078 ± 0.079	-0.012 ± 0.011	0.023 ± 0.001	0.75	-0.045 ± 0.015
1.386	0.54	6.47	7.0	0.305 ± 0.083	0.052 ± 0.017	0.021 ± 0.001	0.76	0.041 ± 0.022
1.527	0.52	6.47	7.0	0.392 ± 0.088	0.069 ± 0.017	0.015 ± 0.001	0.83	0.065 ± 0.021
1.623	0.51	6.47	7.0	0.233 ± 0.156	0.042 ± 0.028	0.015 ± 0.002	0.83	0.033 ± 0.033
1.709	0.49	6.47	7.0	0.305 ± 0.086	0.045 ± 0.014	0.013 ± 0.001	0.85	0.038 ± 0.016
1.824	0.48	6.47	7.0	0.451 ± 0.122	0.075 ± 0.021	0.014 ± 0.001	0.83	0.074 ± 0.026
1.419	1.56	9.71	8.0	-0.165 ± 0.256	-0.024 ± 0.045	0.015 ± 0.003	0.89	-0.045 ± 0.052
1.512	1.54	9.71	8.0	0.828 ± 0.215	0.130 ± 0.037	0.010 ± 0.002	0.92	0.130 ± 0.040
1.613	1.51	9.71	8.0	0.724 ± 0.146	0.095 ± 0.025	0.009 ± 0.001	0.93	0.093 ± 0.027
1.716	1.48	9.71	8.0	0.710 ± 0.170	0.095 ± 0.026	0.007 ± 0.002	0.95	0.093 ± 0.027
1.794	1.45	9.71	8.0	0.070 ± 0.365	0.000 ± 0.056	0.007 ± 0.004	0.95	-0.007 ± 0.059

(f^e) is the fraction of the events due to inelastic (elastic) scattering (Table I). The fractions f are deduced from a parametrization of unpolarized cross-section data⁷ equivalently radiated⁸ for our target thickness of 0.1 radiation length. The radiative corrections due to contaminations from inelastic domains appear in Table II. Contributions from inside the W bin under consideration (f_{cuts}) were treated as the true signal from which the radiatively corrected asymmetries were formed.⁹ The statistical errors in the asymmetries are increased by factors of 1–1.6 because (0–60)% of the events originated outside the W cuts.

The completely corrected results are given in Table II with variables the same as those defined in Ref. 2. The depolarizing factor D depends on

the value of $R = \sigma_L/\sigma_T$ taken to be 0.1.¹⁰ In addition to the electron asymmetry A , we show the resulting virtual-photon-proton asymmetry $A/D = A_1 + \eta A_2$, where $A_1 = (\sigma_{1/2} - \sigma_{3/2})/(\sigma_{1/2} + \sigma_{3/2})$, with $\sigma_{1/2}$ ($\sigma_{3/2}$) the total absorption cross section for the net spin component of the virtual photon plus proton along the photon direction of motion equal to $\frac{1}{2}$ ($\frac{3}{2}$). The quantity ηA_2 is an interference term bounded by $|A_2| \leq R^{1/2}$. The uncertainties shown are dominated by statistical errors.

The radiatively corrected values of $A/D = A_1 + \eta A_2$ from Table II are plotted versus W in Fig. 1(a) with two previously published data points also shown just outside the resonance region.³ Except in the region of the $\Delta(1232)$ resonance, the values of $A_1 + \eta A_2$ are predominantly large and positive throughout the entire range in W . Ex-

TABLE II. Inelastic radiative corrections and completely corrected electron and photon asymmetry results.

Range of W (GeV)	W (GeV)	Q ² (GeV/c) ²	A (Corrected electron asymmetry)	D (for R = 0.1)	A ₁ + ηA ₂ (Corrected photon asymmetry)	Inelastic Radiative Correction(a)	ηA ₂ (Upper limit for R = 0.1)	f _{cuts} ^(b)	f _{bkgd} ^(c)
1.090–1.184	1.168	0.57	-0.030 ± 0.074	0.088	-0.34 ± 0.83	0.00	0.38	1.00	0.35
1.184–1.312	1.247	0.56	-0.045 ± 0.017	0.103	-0.44 ± 0.16	0.00	0.32	0.92	0.26
1.312–1.472	1.386	0.54	0.067 ± 0.034	0.132	0.50 ± 0.26	+0.20	0.24	0.65	0.64
1.472–1.584	1.527	0.52	0.082 ± 0.031	0.165	0.49 ± 0.18	+0.10	0.19	0.68	0.58
1.584–1.648	1.623	0.51	0.042 ± 0.065	0.191	0.22 ± 0.34	+0.04	0.16	0.51	0.76
1.648–1.776	1.709	0.49	0.045 ± 0.027	0.215	0.21 ± 0.12	+0.03	0.14	0.61	0.70
1.776–1.872	1.824	0.48	0.094 ± 0.053	0.250	0.38 ± 0.21	+0.08	0.12	0.48	0.89
1.360–1.472	1.419	1.56	-0.017 ± 0.077	0.152	-0.11 ± 0.51	+0.18	0.24	0.67	0.76
1.472–1.552	1.512	1.54	0.151 ± 0.057	0.166	0.91 ± 0.35	+0.12	0.22	0.69	0.59
1.552–1.664	1.613	1.51	0.113 ± 0.043	0.183	0.62 ± 0.23	+0.11	0.19	0.63	0.81
1.664–1.776	1.716	1.48	0.103 ± 0.041	0.201	0.51 ± 0.21	+0.05	0.17	0.65	0.72
1.776–1.840	1.794	1.45	-0.035 ± 0.148	0.216	-0.16 ± 0.69	-0.13	0.16	0.40	0.87

^a $(A_1 + \eta A_2)^{\text{corr}} - (A_1 + \eta A_2)^{\text{uncorr}}$.

^b Fraction of events inside cuts, used for inelastic radiative corrections.

^c Fraction of nonresonant background present in corrected asymmetries.

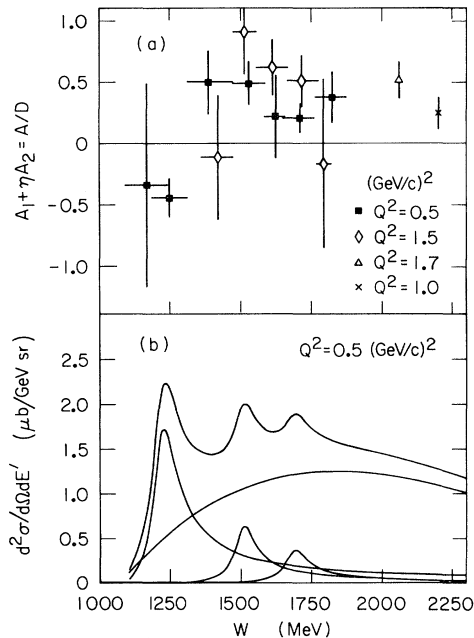


FIG. 1. (a) Asymmetry vs missing mass W . (b) Differential cross section vs W . Also shown is a decomposition into individual resonances and the background.

traction of values for individual resonances is complicated by the presence of a large nonresonant background, as is easily seen from Fig. 1(b) which shows all the contributions at $Q^2 = 0.5$ (GeV/c^2). The proportion of inelastic events not due to the resonances is given in the last column of Table II.

The contribution to the asymmetry $A_1 + \eta A_2$, which arises from the two channels $ep \rightarrow e\eta\pi^+$ and $ep \rightarrow e\pi\pi^0$, has been calculated¹¹ for our kinematic points. This calculation is based on a multipole analysis¹² of extensive electroproduction data in the resonance region and does not use our data. The results of these calculations are displayed in Fig. 2 for the cases of Born-term asymmetries alone (curve *a*), Born-term plus $\Delta(1232)$ asymmetries (curve *b*), and Born-term plus all resonance asymmetries (curve *c*). It is not surprising that curve *a* shows asymmetries beginning near zero at low W instead of near +1 (which an s -wave assumption would dictate) since the presence of the charged channels requires¹³ the retention of the pion pole term (which contains all partial waves). Thus angular-momentum-barrier arguments are ruled out, even this close to threshold. Although single-pion electroproduction accounts for only about one-half of the total inelastic cross section in our kinematic region, good agreement

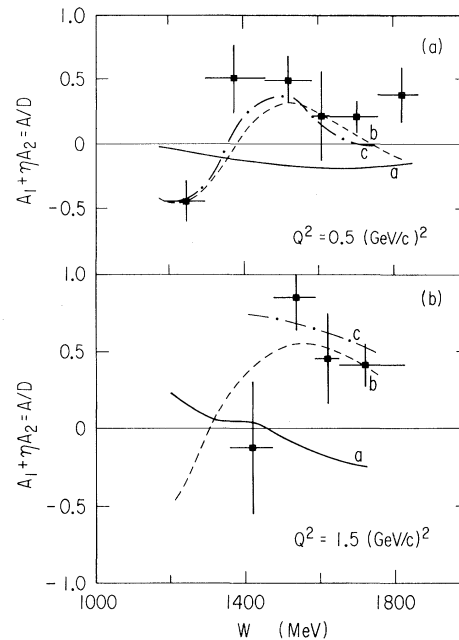


FIG. 2. (a) Asymmetry data at $Q^2 \approx 0.5$ (GeV/c^2) compared with a multipole analysis performed by Devenish and Gerhardt: curve *a*, Born terms alone; curve *b*, Born terms plus $\Delta(1232)$; and curve *c*, Born terms plus all resonances. (b) Same for $Q^2 \approx 1.5$ (GeV/c^2).

is obtained with our data. Thus the net asymmetry contributed by the other channels cannot be very different from our measured asymmetries.

At the center of the $\Delta(1232)$, the dominant A_1 component of A/D is expected to be -0.5 for the P_{33} partial wave, which is known to be essentially pure $M1$ excitation and which contributes 74% to our datum point at $W = 1.240$ GeV. The P_{33} partial wave is still very strong throughout the second and third resonance peaks, but the associated asymmetry changes sign outside the central region of the first resonance, as shown by curve *b* in Fig. 2.

Theoretical predictions about the asymmetry of the $D_{13}(1520)$ and $F_{15}(1688)$ resonance are more uncertain. Symmetric quark models,¹⁴ for example, predict a rapid change of the asymmetry from negative to positive as Q^2 varies from 0.5 to 1.5 (GeV/c^2). As a consequence of the strong nonresonant background more precise asymmetry data are required for the isolation of these individual resonance asymmetries.

The global effect of the spin-dependent behavior of all the s -channel resonances has been studied in the framework of a symmetrical quark model.¹⁵ Somewhat surprisingly, the polariza-

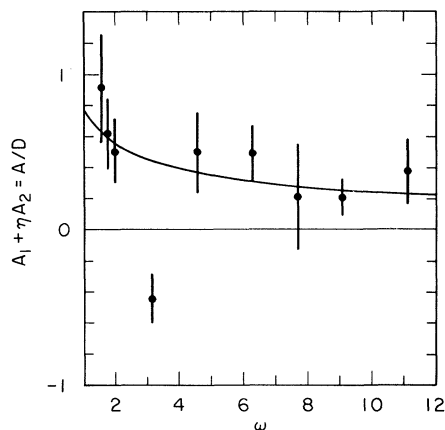


FIG. 3. Asymmetry vs scaling variable ω . The curve $0.78\omega^{-1/2}$ is a fit to deep-inelastic data ($W > 2$ GeV). The data points are the resonance-region results ($W < 2$ GeV) of this work.

tion asymmetry of the summed resonances duplicates the result of the naive quark model for the deep inelastic region ($A_1 = \frac{5}{9}$). The resonance-region asymmetries must be predominantly negative in the photoproduction limit ($Q^2 = 0$), as can be inferred from the Drell-Hearn-Gerasimov sum rule,¹⁶ and our data show that the asymmetry has already changed sign at $Q^2 = 0.5$ (GeV/c)². In the unpolarized case, it is well known that the structure function νW_2 scales, when locally averaged, even throughout much of the resonance region, and that at least a form of global duality holds between the resonance region and the deep inelastic region.¹⁷ In order to test whether such a correspondence exists in the polarized case as well, we have plotted in Fig. 3 our resonance data against the scaling variable $\omega = 2M\nu/Q^2$. The curve shown ($0.78\omega^{-1/2}$) is a fit to our deep-inelastic data.³ At the first resonance, a major oscillation away from the deep-inelastic curve occurs, but otherwise scaling seems to apply for all resonance points. The situation does not change if we use slightly different scaling variables which have been suggested.¹⁷ We conclude that the spin-dependent behavior is also consistent with a duality mechanism, in analogy to the unpolarized case.

We are indebted to R. Devenish and V. Gerhardt for the multipole calculations. We also thank R. Devenish and F. Gilman for valuable discussions. The research was supported in part by the

U. S. Department of Energy under Contracts No. DE-AC02-76ER03075 and No. DE-AC03-76SF-00515, the German Federal Ministry of Research and Technology, and the Japan Society for the Promotion of Science. One of us (V.W.H.) was a recipient of a John Simon Guggenheim Memorial Foundation Fellowship 1978-1979.

(a) Present address: Cornell University, Ithaca, N. Y. 14850.

(b) Present address: University of California, Santa Barbara, Cal. 93106.

(c) Present address: Kyoto University, Kyoto 606, Japan.

¹M. J. Alguard *et al.*, Phys. Rev. Lett. **37**, 1258 (1976).

²M. J. Alguard *et al.*, Phys. Rev. Lett. **37**, 1261 (1976).

³M. J. Alguard *et al.*, Phys. Rev. Lett. **41**, 70 (1978).

⁴M. R. Bergström *et al.*, Bull. Am. Phys. Soc. **23**, 529 (1978).

⁵G. Baum *et al.*, in Proceedings of the Twentieth International Conference on High Energy Physics, Madison, Wisconsin, July 1980 (to be published).

⁶K. P. Schüller, in *High Energy Physics with Polarized Beams and Polarized Targets*, Argonne, 1978, edited by G. H. Thomas, AIP Conference Proceedings No. 51 (American Institute of Physics, New York, 1979), p. 217.

⁷S. Stein *et al.*, Phys. Rev. D **10**, 1884 (1975).

⁸L. W. Mo and Y.-S. Tsai, Rev. Mod. Phys. **41**, 205 (1969); Y.-S. Tsai, SLAC Report No. SLAC-PUB-848, 1971 (unpublished).

⁹M. R. Bergström, Ph.D. thesis, Yale University, 1979 (unpublished).

¹⁰F. W. Brasse *et al.*, Nucl. Phys. **B110**, 413 (1976).

¹¹R. C. E. Devenish and V. Gerhardt, private communication.

¹²R. C. E. Devenish and D. H. Lyth, Nucl. Phys. **B93**, 109 (1975).

¹³R. L. Walker, Phys. Rev. **182**, 1729 (1969).

¹⁴F. Ravndal, Phys. Rev. D **4**, 1466 (1971); S. Ono, Nucl. Phys. **B107**, 522 (1976); for a dual model, see J. G. Körner, DESY Report No. DESY-75/57, 1975 (unpublished).

¹⁵F. E. Close *et al.*, Phys. Rev. D **6**, 2533 (1972); F. E. Close and F. J. Gilman, Phys. Rev. D **7**, 2258 (1973).

¹⁶S. D. Drell and A. C. Hearn, Phys. Rev. Lett. **16**, 908 (1966); S. B. Gerasimov, Sov. J. Nucl. Phys. **2**, 430 (1966); I. Karliner, Phys. Rev. D **7**, 2717 (1973).

¹⁷E. D. Bloom and F. J. Gilman, Phys. Rev. D **4**, 2901 (1971); V. Rittenberg and H. R. Rubinstein, Phys. Lett. **35B**, 50 (1971).